It is also important to investigate the influence of the upgraded data set (*2*), sampling, and model uncertainties on our conclusions. In all our results, we use a sampling strategy that compares model and observations only where observations exist; we do not use the infilled or interpolated data set (*11*). As a test, however, we repeated the analysis using the infilled data and found that it made no difference to the conclusions. More details on these sampling issues are found in (*16*). We also estimated the impact that model errors might have on the results. Multiple models run with the same GHG forcing (*25*) show a factor of 2 difference in ocean basin heat content after 80 years of integration (*26*, *27*). We estimated the effect that this had in the detection scheme and still found robust detection results above the level of natural variability (*16*). Therefore, the conclusion that the observed ocean warming is due to human influences is robust to major perturbations of both the observed data set and model error.

The implications of our results go far beyond identifying the reasons for ocean warming. First, they show that uncertainties in the models used here are too small to affect the conclusion attributing the historic ocean warming signal to anthropogenic forcings, at least for the temperature-driven part of the signal. Second, taking these new results with those obtained in the last few years [e.g., (*1*, *28*–*30*); see earlier detection studies cited above] leaves little doubt that there is a human-induced signal in the environment. Third, because the historical changes have been well simulated, future changes predicted by these global models are apt to be reasonably good, at least out to, say, 20 to 30 years into the future. How to respond to the serious problems posed by these predictions is a question that society must decide.

References and Notes

1. IPCC, "WG1 Third Assessment Report," J. T. Houghton *et al.* Eds. (2001).
2. S. Levitus, J. Antonov, T. Boyer, *Geophys. Res. Lett.* **32**, L02604, doi:10.1029/2004GL021592 (2005).
3. T. P. Barnett, D. W. Pierce, R. Schnur, *Science* **292**, 270 (2001).
4. S. Levitus *et al.*, *Science* **292**, 267 (2001).
5. B. K. Reichert, R. Schnur, L. Bengtsson, *Geophys. Res. Lett.* **29**, 1525 (2002).
6. J. Hansen *et al.*, *J. Geophys. Res.* **107** (D18), 4347 (2002).
7. J. M. Gregory, H. T. Banks, P. A. Stott, J. A. Lowe, M. D. Palmer, *Geophys. Res. Lett.* **31**, L15312 (2004).
8. P. R. Gent, G. Danabasoglu, *J. Clim.* **17**, 4058 (2004).
9. W. M. Washington *et al.*, *Clim. Dyn.* **16**, 755 (2000).
10. C. Gordon *et al.*, *Clim. Dyn.* **16**, 147 (2000).
11. Methods are available as supporting material on *Science* Online.
12. G. C. Hegerl *et al.*, *J. Clim.* **9**, 2281 (1996).
13. G. C. Hegerl *et al.*, *Clim. Dyn.* **13**, 613 (1997).
14. M. R. Allen, S. F. B. Tett, *Clim. Dyn.* **15**, 419 (1999).
15. K. Hasselmann, *Clim. Dyn.* **13**, 601 (1997).
16. D. W. Pierce *et al.*, in preparation.
17. G. A. Meehl, W. M. Washington, T. M. L. Wigley, J. M. Arblaster, A. Dai, *J. Clim.* **16**, 426 (2003).
18. A. Dai, W. M. Washington, G. A. Meehl, T. W. Bettge, W. G. Strand, *Clim. Change* **62**, 29 (2004).
19. G. Neumann, W. J. Pierson, *Principles of Physical Oceanography* (Prentice-Hall, NJ, 1966).
20. M. J. McPhaden, D. Zhang, *Nature* **415**, 603 (2002).
21. V. Ramanathan *et al.*, *J. Geophys. Res.* **106**, 28,371 (2001).
22. V. Ramanathan *et al.*, in preparation.
23. T. Lee, *Geophys. Res. Lett.* **31**, L18305 (2004).
24. S. F. B. Tett, P. A. Stott, M. R. Allen, W. J. Ingram, J. F. B. Mitchell, *Nature* **399**, 569 (1999).
25. CMIP2+ runs are available at http://www-pcmdi.llnl.gov.
26. A. P. Sokolov, C. E. Forest, P. H. Stone, *J. Clim.* **16**, 1573 (2003).
27. K. M. AchutaRao *et al.*, in preparation.
28. B. D. Santer *et al.*, *Science* **301**, 479 (2003).
29. B. D. Santer *et al.*, *J. Geophys. Res.* **109**, D21104 (2004).
30. B. D. Santer, J. E. Penner, P. W. Thorne, in *Temperature Trends in the Lower Atmosphere: Steps for Understanding and Reconciling Differences* (Report by the U.S. Climate Change Science Plan and the Subcommittee on Global Change Research, Washington, DC, in press).

31. This work is a contribution from the International Detection and Attribution Group funded by the National Oceanic and Atmospheric Association (NOAA) and the U.S. Department of Energy (DOE) through NOAA's CCDD program. We gratefully acknowledge DOE support through grants DE-FG03-01ER63255 to the Scripps Institute of Oceanography and DOE-W-7405-ENG-48 to the Program for Climate Model Diagnoses and Intercomparison at Lawrence Livermore National Labatory. Work at the Hadley Centre was supported by the UK Department for Environment, Food and Rural Affairs under contract PECD 7/12/37 and by the Government Meteorological Research and Development Programme. We especially thank S. Levitus for making his new ocean data set available and colleagues at NCAR and the Hadley Centre for performing and making available the model runs used in this work. Computer time for the PCM simulations was provided by the National Center for Atmospheric Research Scientific Computing Division, the DOE National Energy Research Scientific Computing Center, Oak Ridge National Laboratory, and the Los Alamos National Laboratory's Advanced Computing Laboratory. Discussions with L. Talley and R. Davis were helpful in several aspects of the study.

Supporting Online Material

www.sciencemag.org/cgi/content/full/1112418/DC1
Materials and Methods
SOM Text
Figs. S1 and S2
References and Notes

17 March 2005; accepted 12 May 2005
Published online 2 June 2005;
10.1126/science.1112418
Include this information when citing this paper.

Ecosystem Collapse in Pleistocene Australia and a Human Role in Megafaunal Extinction

Gifford H. Miller,[1] Marilyn L. Fogel,[2] John W. Magee,[3] Michael K. Gagan,[4] Simon J. Clarke,[5] Beverly J. Johnson[6]

Most of Australia's largest mammals became extinct 50,000 to 45,000 years ago, shortly after humans colonized the continent. Without exceptional climate change at that time, a human cause is inferred, but a mechanism remains elusive. A 140,000-year record of dietary $\delta^{13}C$ documents a permanent reduction in food sources available to the Australian emu, beginning about the time of human colonization; a change replicated at three widely separated sites and in the marsupial wombat. We speculate that human firing of landscapes rapidly converted a drought-adapted mosaic of trees, shrubs, and nutritious grasslands to the modern fire-adapted desert scrub. Animals that could adapt survived; those that could not, became extinct.

Humans are thought to have colonized Australia between 55 and 45 thousand years ago (ka) (*1*–*5*), and most of its large animals became extinct between 50 and 45 ka (*6*, *7*). The 60 taxa known to have become extinct include all large browsers, whereas large grazing forms, such as red and gray kangaroos, were less affected. The selective loss of large browse-dependent taxa suggests that ecosystem change may have been important, although animal size may have played a role (*8*). Inferential evidence of vegetation reorganization and a changed fire regime beginning 45 ka is recorded in terrestrial (*9*, *10*) and marine (*11*, *12*) sediment cores. But no records of ecosystem status through this time interval are available from the vast semiarid zone. We used isotopic tracers of diet preserved in avian eggshells and marsupial teeth (*13*, *14*) to monitor ecosystems before and after human colonization. These dietary reconstructions document ecosystem collapse across the semiarid zone between 50 and 45 ka.

We recovered eggshells of the Australian emu *Dromaius novaehollandiae* and the extinct giant flightless bird *Genyornis newtoni* from longitudinal desert dunes and shoreline-

[1]INSTAAR and Geological Sciences, University of Colorado, Boulder, CO 80309–0450 USA. [2]Geophysical Laboratory, Carnegie Institution of Washington, 1051 Broad Branch Road, Washington, DC 20015, USA. [3]Department of Earth and Marine Sciences, [4]Research School of Earth Sciences, Australian National University, Canberra, ACT 0200, Australia. [5]Charles Sturt University, Locked Bag 588, Wagga Wagga, NSW 2678, Australia. [6]Department of Geology, Bates College, Lewiston, ME 04240–6028, USA.

marginal dunes around Lake Eyre (LE), the terminal playa of a large interior basin in central Australia (Fig. 1). These collections were supplemented by eggshell remains collected near Port Augusta (PA) and the Darling-Murray lakes (DM) (Fig. 1). Because the eggshells are fragmented, we grouped most shells into collections taken from locations separated by 100 m or more to avoid analyzing multiple fragments from the same egg. Temporal constraints are based on ^{14}C dates on eggshell (LE, n = 111 samples; PA and DM, n = 60), luminescence ages on sand grains enclosing eggshells found in eolian deposits >40,000 years old (n = 28, table S5), and amino acid racemization (AAR) in eggshell organic matter for all eggshells in which we measured isotopic ratios (LE, n = 893; PA, n = 276; DM, n = 220). AAR measurements were converted to calendar ages using an age model derived from ^{14}C and luminescence dates; of 191 LE *Dromaius* eggshells <45,000 years old, 84 were dated by ^{14}C analyses. All ^{14}C-dated *Genyornis* eggshells (n = 18) are beyond the reliable age of radiocarbon dating; for LE, they were plotted against calibrated AAR ages.

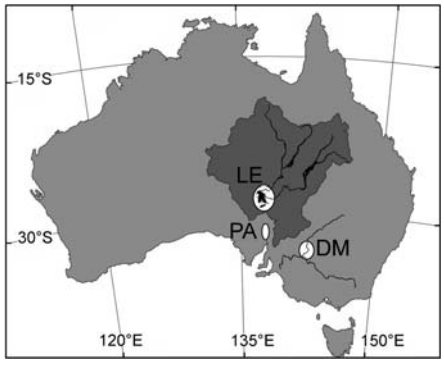

Fig. 1. Map of Australia, showing the Lake Eyre Basin (dark gray) and primary collecting localities around Lake Eyre (LE, black), Port Augusta (PA), and the Darling-Murray Lakes (DM), which include the Minindee, Annabranch, and Willandra Lakes; the Perry Sand Hills; and Lake Victoria.

We reconstructed paleodiets for *Dromaius* and *Genyornis* based on the carbon isotopic composition ($\delta^{13}C$) of their eggshells (tables S1 to S3). Bird eggshells are a calcite biomineral containing 3% organic matter, most of which is sequestered within the calcite crystals of the eggshell, where it is stable in the geological environment for >10^6 years (*15*). The isotopic composition of carbon in eggshell organic residues ($\delta^{13}C_{org}$) and in the calcite matrix ($\delta^{13}C_{carb}$) is determined by the $\delta^{13}C$ of the birds' diet, offset by systematic biochemical fractionation (*16*, *17*). Most plants use either the C_3 or C_4 photosynthetic pathways, which around LE yield average $\delta^{13}C$ values of –26.3 ± 2.1 per mil (‰) and –13.7 ± 0.7‰ (table S6). Crassulacean acid metabolism plants rarely contribute to *Dromaius* diet. The offset between eggshell $\delta^{13}C_{org}$ and the $\delta^{13}C$ values of food sources is 3‰ (*18*), which is similar to that observed in controlled feeding experiments (*17*). The average offset between $\delta^{13}C_{carb}$ and $\delta^{13}C_{org}$ in *Dromaius* eggshell is 10.4 ± 2.0‰ (n = 269), whereas the offset is 11.1 ± 1.5‰ (n = 127) for *Genyornis*, after adjusting for biases due to apparent summer breeding (*18*). Each eggshell records conditions during a single season. Calcite carbon, derived from blood, reflects food sources in the days to weeks before egg-laying (*16*). In contrast, eggshell organic residues are derived from protein sources and reflect both recent and potentially older protein reserves, integrating dietary intake over several months.

Dromaius lives across the Australian mainland, nesting in the austral winter throughout its range. Our 140,000-year dietary reconstruction for *Dromaius* from LE is based on $\delta^{13}C_{org}$

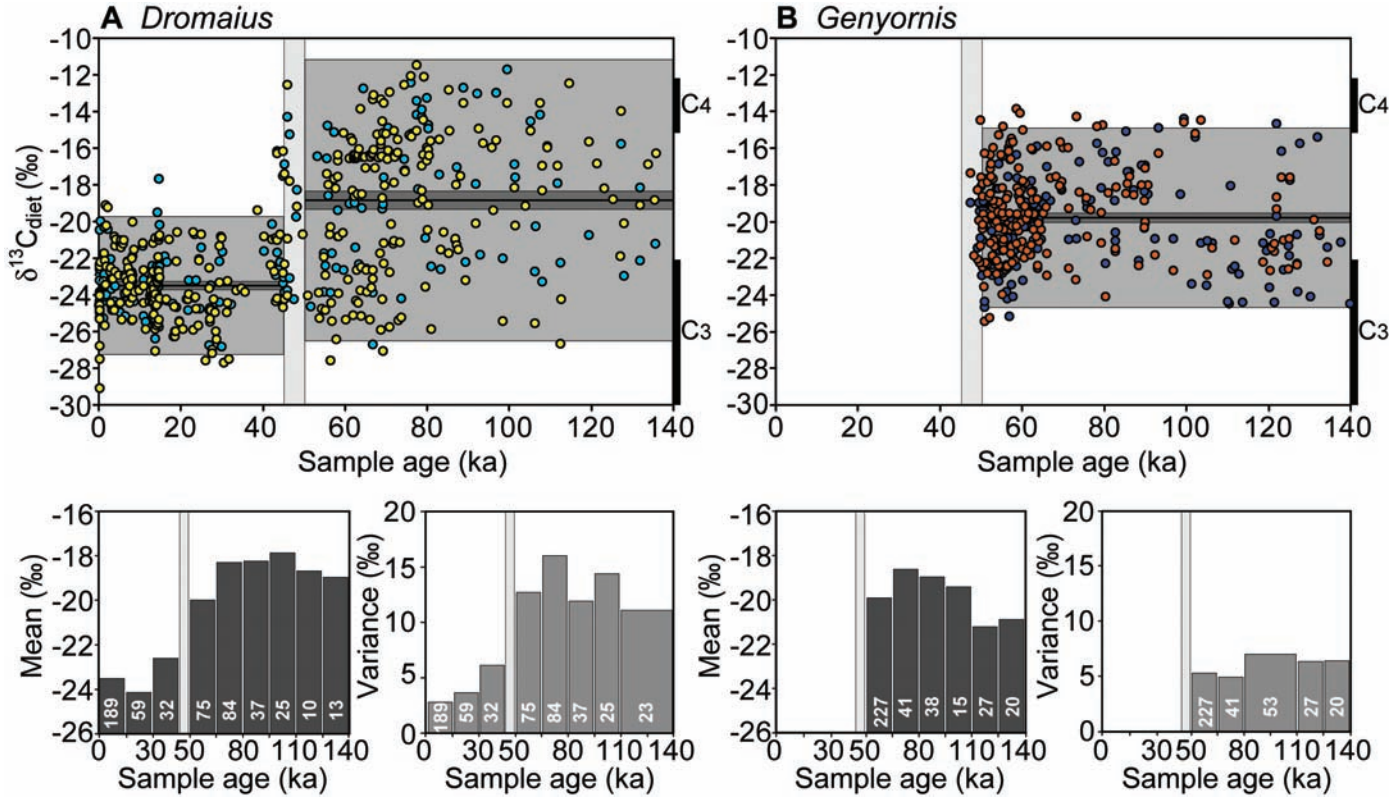

Fig. 2. Time series of *Dromaius* (**A**) and *Genyornis* (**B**) dietary $\delta^{13}C$ reconstructed from $\delta^{13}C_{carb}$ (light colors) and $\delta^{13}C_{org}$ (dark colors) of individually dated eggshells from the LE region (Fig. 1). The vertical bars (50 to 45 ka) define the megafaunal extinction window, with its estimated uncertainty. Measured $\delta^{13}C_{org}$ and $\delta^{13}C_{carb}$ values were converted to dietary $\delta^{13}C$ by applying biochemical fractionation factors (tables S1 to S3). End-member dietary $\delta^{13}C$ values corresponding to 100% C_3 and 100% C_4 diets (±2σ) are shown on the right. Differences in dietary $\delta^{13}C$ values for the preextinction and postextinction windows are shown by the mean (black line), standard error of the mean (dark gray, 95% confidence), and standard deviation (±2σ, light gray). Bar graphs below each time series show the mean and variance calculated for 15,000-year intervals to test whether climate influenced these statistics significantly. White numbers in each bar denote the number of samples (n) in each interval. Because variance is highly dependent on sample size, we have combined adjacent time windows when n < 20.

(n = 181) and $\delta^{13}C_{carb}$ (n = 344) values in individually dated eggshells (Fig. 2). Between 50 and 45 ka, mean dietary $\delta^{13}C$ decreased by at least 3.4‰ (95% confidence level), accompanied by an even larger decrease in dietary variance, from 14.8 to 3.8‰ (Fig. 2). Before 50 ka, *Dromaius* ate a wide range of food sources, ranging from a nearly pure C_4 diet to a nearly pure C_3 diet, with almost any combination of intermediate feeding strategies. This $\delta^{13}C$ distribution is consistent with an opportunistic feeder that lived in an environment with high interannual moisture variability. The isotopic data imply that *Dromaius* utilized abundant nutritious grasslands in wet years (C_4), relying more on shrubs and trees in drier years (C_3). After 45 ka, *Dromaius* utilized a restricted range of food sources, dominated by C_3 plants.

Frequency histograms of *Dromaius* dietary $\delta^{13}C$ (Fig. 3) provide clues about the nature of past ecosystems around LE. Before 50 ka, $\delta^{13}C$ dietary tracers reflect a weakly bimodal pattern, with a broad dominance of C_4 dietary sources and a subsidiary peak dominated by C_3 plants. Two-thirds of both dietary tracers reflect >50% C_4 plant sources, suggesting common nutritious grasslands. In contrast, *Dromaius* living after 45 ka utilized dominantly C_3 dietary sources, always with <50% C_4 plants. Although our dietary reconstructions document increased reliance on C_3 plants by *Dromaius* after 45 ka, the landscape around LE included abundant spinifex and cane grass, C_4 grasses that are largely inedible and low in nutrition and hence a minor component of recent *Dromaius* diets.

To evaluate the possible role of climate in the observed dietary shift, we subdivided the data into 15,000-year intervals back to 140 ka, which includes contrasting climates of the Holocene (15 to 0 ka), the last glacial maximum (30 to 15 ka), and the last interglaciation (125 to 110 ka). The mean and variance of each interval (Fig. 2) are not statistically different from the mean and variance of their larger groupings (>50 and <45 ka), suggesting that climate is not the dominant control on dietary $\delta^{13}C$. The restricted, C_3-dominated dietary range for *Dromaius* after 45 ka persists through the cold, dry, last glacial maximum and the Holocene, when temperatures rose and rainfall increased (*14*, *19*).

The $\delta^{13}C$ values in eggshells of *Genyornis* living around LE between 140 and 50 ka ($\delta^{13}C_{org}$ n = 161; $\delta^{13}C_{carb}$ n = 207; Fig. 2) allow us to compare feeding strategies between a taxon that became extinct and one that survived to the present. *Genyornis* consumed a more restricted diet, exhibiting only 40% of the isotopic variance observed in contemporary *Dromaius*. Frequency histograms of *Genyornis* diet (Fig. 3) are symmetrically distributed and always include some C_4 dietary sources, unlike *Dromaius*, which tolerates a pure C_3 diet. There are no large differences in average dietary $\delta^{13}C$ or in its variance at 15,000-year intervals (Fig. 2), despite large changes in climate (*20*). We conclude that *Genyornis* was a more specialized feeder than *Dromaius*, targeting a specific set of food resources, and that these resources were frequently available through the range of climates between 140 and 50 ka.

To test the inferences derived from the LE data sets, we developed dietary reconstructions using eggshells from two other regions, PA and DM (Fig. 1); both are cooler and wetter than LE. Although both data sets are large, insufficient samples are available to produce time series spanning the past 140,000 years. Luminescence, ^{14}C, and calibrated AAR dates at both sites demonstrate that *Genyornis* extinction and ecosystem change occurred 50 to 45 ka. The lack of any time dependence in the mean or variance in $\delta^{13}C$ for either taxon from LE (Fig. 2) allows firm comparisons between the diets of *Dromaius* and *Genyornis* in age clusters >50 ka and <45 ka for all three regions, without concerns about biasing the statistics by an overrepresentation or absence of data in certain time intervals.

Dietary $\delta^{13}C$ values for *Dromaius* eggshells <45,000 years old from PA and DM reflect almost exclusively C_3 food sources, whereas eggshells >50,000 years old exhibit a greater range in $\delta^{13}C$ values and a higher proportion of C_4 dietary sources (Fig. 3). *Genyornis* dietary $\delta^{13}C$ values exhibit less variance than those of contemporary *Dromaius* and always include some C_4 plants, although in lower proportions (27 to 39%) than at LE (46%). *Genyornis* eggshell $\delta^{13}C$ values show a strong central tendency in both tracers, whereas diets of coexisting *Dromaius* lack a clear central tendency and have greater variance. The results for all three localities are consistent with a substantial reduction in food sources for *Dromaius* 50 to 45 ka and a more specialized feeding strategy for *Genyornis*.

The coeval dietary retraction recorded by *Dromaius* eggshells from three regions widely separated by geography and climate reflects a major disruption in the range of food sources available to the birds about the time of human colonization. If these changes represent a reorganization of vegetation communities across the Australian semiarid zone, we expect to find similar responses in other animal groups. To test this prediction, we measured $\delta^{13}C$ values in hydroxyapatite extracted from wombat tooth enamel from the PA and DM regions (table S4). Wombats are strict herbivores, relying almost exclusively on grasses and reeds. They live, and often die, in sandy deposits used by *Dromaius* and *Genyornis* as breeding sites, and their association with eggshells of known age can date their remains (*18*). Teeth from wombats that lived >50 ka exhibit a wider range of $\delta^{13}C$ values and a much larger proportion of C_4 plants than do teeth of wombats that lived <45 ka (Fig. 3). This difference

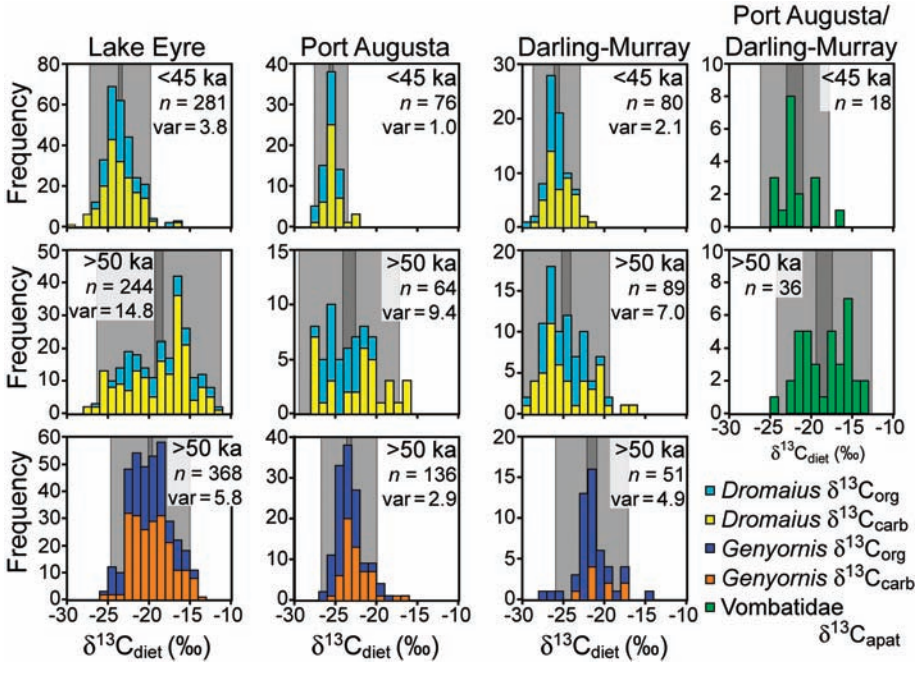

Fig. 3. Frequency histograms of dietary $\delta^{13}C$ for *Dromaius* (middle and top rows) and *Genyornis* (bottom row) from LE, PA, and DM. All sites reveal a shift toward lower mean dietary $\delta^{13}C$ values (95% confidence, dark gray) and reduced spread [$\pm 2\sigma$ (light gray) and variance (var)] after 45 ka. A similar trend is apparent in Vombatidae tooth enamel from PA and DM. *Genyornis* dietary $\delta^{13}C$ always shows less spread and a more consistent proportion of C_4 food sources than does that of coexisting *Dromaius*. Dietary $\delta^{13}C$ is derived from measured $\delta^{13}C_{org}$, $\delta^{13}C_{carb}$, and $\delta^{13}C_{apat}$ (apat, hydroxyapatite) (tables S1 to S4). The number of analyses (n) is shown.

suggests that before 50 ka, C_4 plants made up 40 to 100% of the wombat's dietary intake, whereas after 45 ka, their diet was dominated by C_3 plants, supporting the conclusions derived from *Dromaius* eggshells.

Our eggshell and tooth $\delta^{13}C$ data provide firm evidence for an abrupt ecological shift around the time of human colonization and megafaunal extinction in Australia, about 50 to 45 ka. Climate forcing of the observed vegetation change is unlikely, given that earlier dramatic climate shifts did not result in such a large biotic response and that climate change between 60 and 40 ka was not large, consistent, or sustained. During this interval, the DM region experienced somewhat greater effective moisture, whereas modest drying occurred around LE (*2*, *19*, *20*). A persistently weak Australian monsoon after 45 ka may explain the lack of abundant nutritious C_4 grasses around LE (*14*).

A changed fire regime is another plausible mechanism for ecosystem reorganization. Early human colonizers may have altered the timing and frequency of biomass burning. Humans burn landscapes for many purposes, from clearing passageways and hunting along the fire front, to signaling distant bands and promoting the growth of preferred plants. We speculate that systematic burning practiced by the earliest human colonizers may have converted a drought-adapted mosaic of trees and shrubs intermixed with palatable nutrient-rich grasslands to the modern fire-adapted grasslands and chenopod/desert scrub. Nutrient-poor soils (*21*) may have facilitated the replacement of nutritious C_4 grasses by spinifex, a fire-promoting C_4 grass that is well adapted to low soil nutrient concentrations. A range of C_3 plants may have been lost at the same time, but the isotopic dietary proxy lacks sensitivity to such a loss.

Neither overhunting nor human-introduced diseases, the two most widely cited alternative agents for a human-caused extinction event in Australia, would result in the dramatic changes at the base of the food web documented by our data sets. The reduction of plant diversity apparent in our data, however it came about, would have led to the extinction of specialized herbivores and indirectly to the extinction of their large nonhuman predators. Dietary specialization, rather than feeding strategy (browsing versus grazing), may be the critical extinction predictor. Animals such as *Dromaius*, with wide dietary tolerances, survived the extinction event, whereas more specialized feeders, such as *Genyornis*, became extinct.

References and Notes

1. R. G. Roberts, R. Jones, M. A. Smith, *Nature* **345**, 153 (1990).
2. J. M. Bowler *et al.*, *Nature* **421**, 837 (2003).
3. R. Roberts *et al.*, *Nature* **393**, 358 (1998).
4. C. S. M. Turney *et al.*, *Quat. Geochronol.* **55**, 3 (2001).
5. J. F. O'Connell, J. Allen, *Archaeol. Sci.* **31**, 835 (2004).
6. G. H. Miller *et al.*, *Science* **283**, 205 (1999).
7. R. G. Roberts *et al.*, *Science* **292**, 1888 (2001).
8. C. N. Johnson, G. J. Prideaux, *Austral Ecol.* **29**, 553 (2004).
9. A. P. Kershaw, *Nature* **322**, 47 (1986).
10. C. S. M. Turney *et al.*, *J. Quat. Sci.* **16**, 767 (2001).
11. A. P. Kershaw, P. Moss, S. van der Kaars, *Freshw. Biol.* **48**, 1274 (2003).
12. S. van der Kaars, P. De Deckker, *Rev. Palaeobot. Palynol.* **120**, 17 (2002).
13. P. L. Koch, M. L. Fogel, N. Tuross, in *Stable Isotopes in Ecology and Environmental Science*, K. Lajtha, R. H. Michener, Eds. (Blackwell Scientific, London, 1994), pp. 63–92.
14. B. J. Johnson *et al.*, *Science* **284**, 1150 (1999).
15. G. H. Miller, C. P. Hart, E. B. Roark, B. J. Johnson, in *Perspectives in Amino Acid and Protein Geochemistry*, G. A. Goodfriend, M. J. Collins, M. L. Fogel, S. A. Macko, J. F. Wehmiller, Eds. (Oxford Univ. Press, New York, 2000), pp. 161–181.
16. K. A. Hobson, *Condor* **97**, 752 (1995).
17. B. J. Johnson, M. L. Fogel, G. H. Miller, *Geochim. Cosmochim. Acta* **62**, 2451 (1998).
18. Methods are available as supporting material on *Science* Online.
19. P. P. Hesse, J. W. Magee, S. van der Kaars, *Quat. Int.* **118-119**, 87 (2004).
20. J. W. Magee, G. H. Miller, N. A. Spooner, D. Questiaux, *Geology* **32**, 885 (2004).
21. D. J. Barrett, *Global Biogeochem. Cycles* **16**, 1108 (2002).

22. We thank S. DeVogel, H. Scott-Gagan, N. Spooner, M. Cupper, J. Duncan, and C. Ostertag-Henning for analytical assistance. G.H.M. is responsible for AAR data, M.L.F. and S.J.C. for $\delta^{13}C_{org}$ data, M.K.G. for $\delta^{13}C_{carb}$ data, J.W.M. for site selection, and B.J.J. for eggshell isotope-diet relations. Fieldwork was supported by the U.S. NSF (NSF-ESH) and the Australian Research Council (ARC), and was done with the permission and assistance of local landowners. Analyses were supported by NSF, ARC, and the Australian National University. Assistance in the field provided by P. Clark, S. Webb, G. Atkin, O. Miller, and H. Johnston is gratefully appreciated.

Supporting Online Material

www.sciencemag.org/cgi/content/full/309/5732/287/DC1
Methods
Figs. S1 to S3
Tables S1 to S6
References

22 February 2005; accepted 9 May 2005
10.1126/science.1111288

Stomatal Patterning and Differentiation by Synergistic Interactions of Receptor Kinases

Elena D. Shpak,[1,2]* Jessica Messmer McAbee,[1,2]* Lynn Jo Pillitteri,[1] Keiko U. Torii[1,2]†

Coordinated spacing and patterning of stomata allow efficient gas exchange between plants and the atmosphere. Here we report that three ERECTA (ER)–family leucine-rich repeat–receptor-like kinases (LRR-RLKs) together control stomatal patterning, with specific family members regulating the specification of stomatal stem cell fate and the differentiation of guard cells. Loss-of-function mutations in all three *ER*-family genes cause stomatal clustering. Genetic interactions with a known stomatal patterning mutant *too many mouths* (*tmm*) revealed stoichiometric epistasis and combination-specific neomorphism. Our findings suggest that the negative regulation of ER-family RLKs by TMM, which is an LRR receptor–like protein, is critical for proper stomatal differentiation.

The growth and development of multicellular organisms require both proliferative and asymmetric cell division, the latter of which generates two daughter cells with distinct cell fates. During epidermal development in higher plants, protodermal cells undergo proliferative division to form pavement cells, which protect tissue layers underneath and prevent

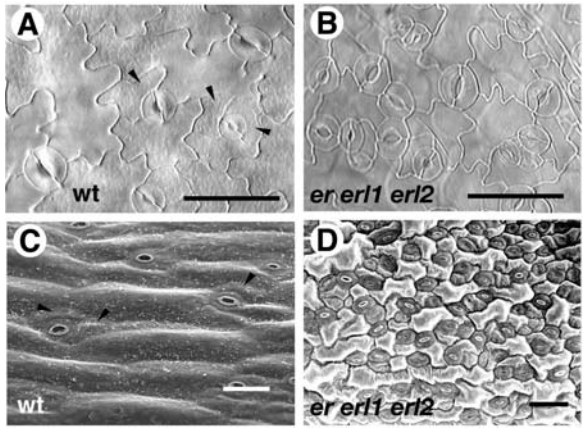

Fig. 1. *ER*-family genes act together in regulating stomatal density and clustering. (**A** and **B**) Cleared differential interference contrast images of abaxial epidermis of a mature rosette leaf of wild type (wt) (A) and *er erl1 erl2* triple mutant (B) leaves. (**C** and **D**) Scanning electron microscopy images of silique epidermis of wild-type (C) and *er erl1 erl2* triple mutant (D) leaves. Overproliferation of stomata and formation of high-density stomatal clusters are evident in the triple mutant. Arrowheads indicate SLGCs. Scale bars in (A) and (B), 50 μm; in (C) and (D), 20 μm.